

# Polyiodine and Polyiodide Species in an Aqueous Solution of Iodine + KI: Theoretical and Experimental Studies

Vincent T. Calabrese and Arshad Khan\*

Chemistry Department, The Pennsylvania State University, DuBois, Pennsylvania 15801

Received: August 11, 1999; In Final Form: October 8, 1999

In the presence of KI, iodine crystals dissolve rapidly in an aqueous solution forming triiodide ions ( $I_3^-$ ) and other neutral species. The experimental evidence does not support the formation of polyiodide ions such as  $I_5^-$ ,  $I_7^-$ , etc. in the solution. However, there is a strong evidence suggesting the formation of polyiodine species,  $I_{2x}$ , where  $x = 2, 3$ , etc., stabilized by  $H^+$  ions in the solution. Ab initio results are presented for structures and energies of some of these species with an  $x$  value of up to 4. Each geometry optimization was done at the HF/LANL2DZ level followed by a single-point energy calculation at the MP2/LANL2DZ level. These calculations suggest that the isolated polyiodine species are not stable and, among the complexed species, the protonated clusters are most stable.

## Introduction

It is a common observation that the solubility of iodine crystals in water is remarkably increased when KI is added to the solution. It is believed by many that the polyiodide ions such as  $I_3^-$ ,  $I_5^-$ ,  $I_7^-$ , etc., form in the aqueous solution<sup>1–6</sup> and take part in the formation of blue amylose iodine (AI) or more commonly known as starch–iodine complex. While a number of researchers considered the involvement of  $I_3^-$  ions with the complex,<sup>1,2</sup> others considered the involvement of  $I_5^-$  ions,<sup>3–5</sup>  $I_7^-$  ions,<sup>6</sup> or species without any  $I^-$  ions.<sup>6,7</sup> Because of the lack of direct experimental results, the above controversy remained undiminished until very recently. Our recent experiment<sup>8</sup> with an iodide ion selective electrode (ISE) suggests that the iodide ions are not consumed in the AI complex forming reaction even when these ions are present in the solution. This finding suggests that the iodide ions are not required for the AI complex formation and, hence, one can ignore the possible involvement of  $I_3^-$ ,  $I_5^-$ , and  $I_7^-$  species with the complex.

To the best of our knowledge, the original consideration of these species, especially the larger ones, like  $I_5^-$  and  $I_7^-$  in the solution stemmed from the AI complex forming chemistry, and in view of the above ISE results it became necessary to re-examine the presence of polyiodide ions in the solution. It should be pointed out that the polyiodide ions such as  $I_3^-$  and  $I_5^-$  are known to exist<sup>9–14</sup> in solid crystal structures. However, their existence in aqueous solutions has never been confirmed. Even though the gas-phase theoretical studies predict significant stability for each of the  $I_3^-$  and  $I_5^-$  ions (relative to separated constituent molecules and ions),<sup>15</sup> it is not known whether they can survive frequent collisions with solvent molecules in the solution. In an aqueous solution, the following reactions can be considered for the formation of large polyiodide species,



In this paper, possible formation of the above iodide species has been investigated. The first part of the paper describes

experimental results that establish the existence of only  $I_3^-$  ions among the possible anionic iodide species, and provides evidence for polyiodine species such as  $I_4$ ,  $I_6$ ,  $I_8$ , etc. stabilized by  $H^+$  ions in the solution. In the second part, the ab initio results that establish the structure and stability of the above polyiodine species are discussed.

## Experimental Evidence for $I_3^-$ Ions and Polyiodine Species

**Absorbance Peaks at 350 and 460 nm and Species Involved.** The absorbance spectra were taken from 300 to 700 nm by using a Spectronic 601 spectrophotometer. Figure 1 represents spectra of solutions (15 °C) containing  $I_2$  and  $I^-$  concentration (molarity) ratios of 0:1, 1:0, 1:1/4, 1:1/2, 1:1, and 1:3 for a fixed  $I_2$  concentration of  $2.0 \times 10^{-4}$  M. The 0:1 ratio had no  $I_2$ , and the  $I^-$  concentration was  $2.0 \times 10^{-4}$  M. For pure  $I^-$  (from KI) ion solution (0:1), a horizontal line was obtained without any absorbance peak and for pure  $I_2$  solution (1:0) a broad peak at around 460 nm was noticed with a very small peak at around 350 nm. As the  $I^-$  proportion was increased in the solution, the absorbance value at 350 nm was increased and that at 460 nm decreased. At a large proportion of  $I^-$  (1:3, uppermost curve of Figure 1) ions, the 460 nm peak completely disappeared and a significant peak intensity was noticed at 350 nm. This observation suggests that the peak intensity at 350 and 460 nm must be due to iodide (may be due to  $I_3^-$ ,  $I_5^-$ ,  $I_7^-$ , etc.) and iodine species (may be due to  $I_2$ ,  $I_4$ ,  $I_6$ , etc.), respectively. At a very low iodine concentration (without any added  $I^-$ ), it is unlikely that iodine species larger than  $I_2$  ( $I_4$ ,  $I_6$ , etc., requires two, three, etc. iodine molecules) can form. Since the same straight-line relationship (Figure 2) is maintained from very low to high iodine concentration, the 460 nm absorbance is expected to be due to  $I_2$  or species that contain  $I_2$  molecules.

**Identifying Anionic Species at 350 nm.** To determine the composition of iodide species at 350 nm, we used pure iodine and KI solutions of the same concentration ( $2.6 \times 10^{-4}$  M  $I_2$  or  $I^-$ ) and applied Job's method of continuous variation. The absorbance readings were taken for mixed solutions of  $I_2$  and  $I^-$  with volumes (mL) of (0:10), (1:9), (2:8), (3:7), (4:6), (5:5), (6:4), (7:3), (8:2), (9:1) and (10:0). Since pure iodine (10:0)

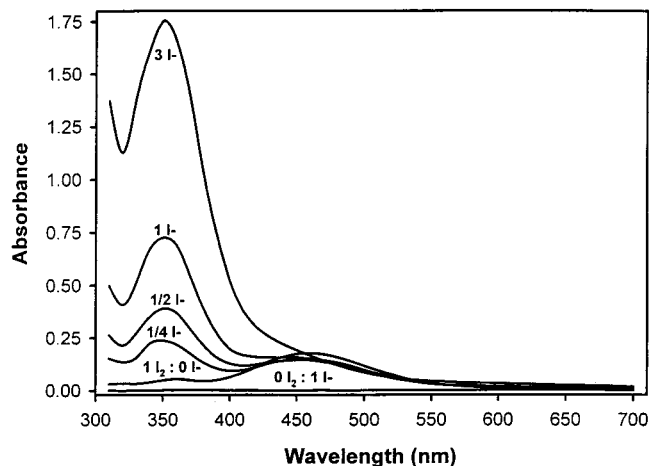


**Figure 1.** Absorption spectra (15 °C) for solutions containing different proportions of iodine and iodide ions. The  $I_2/I^-$  ratios presented in the figure are 0:1, 1:0, 1:1/4, 1:1/2, 1:1, and 1:3 (upper most curve). Except in the 0:1 ratio (where no iodine was added), the iodine concentration was fixed at  $2.0 \times 10^{-4}$  M in each solution.

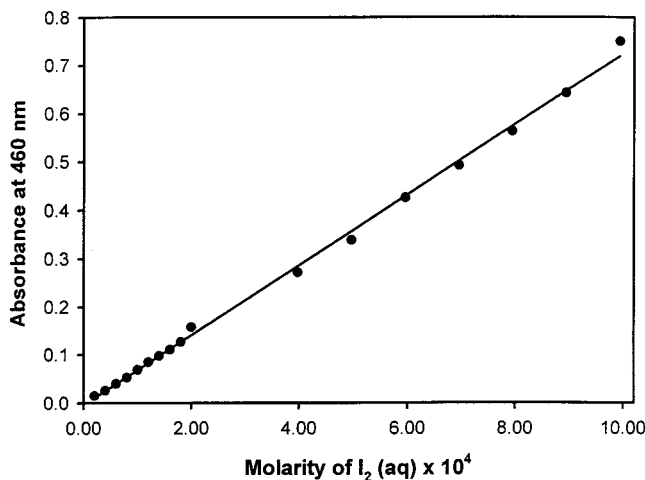


**Figure 2.** Molarity of  $I_2$  against its absorbance at 460 nm shown. This straight-line plot passes through the origin, suggesting that the absorbance at 460 nm goes to zero as the iodine concentration approaches zero.

shows weak absorbance (around 0.04) at 350 nm, we subtracted iodine contribution (after multiplying 0.04 with volume ratios of 0:10, 1:10, 2:10, 3:10, ... 10:10) from each data point so as to obtain absorbance due to anionic iodide species only. Figure 3 shows milliliters of iodine (KI volume = 10 - mL iodine) vs absorbance plot (350 nm) for experiments at 15 °C. The peak position corresponds to 1:1 ( $I_2/I^-$ ) composition for iodide species and, hence, represents the anionic  $I_3^-$  ions (one  $I_2$  and one  $I^-$  ion) that absorb at 350 nm. If  $I_5^-$  or  $I_7^-$  ions also absorbed at 350 nm, the peak position of Figure 3 would not have been at 1:1. For example, if only the  $I_5^-$  or  $I_7^-$  ions were present in the solution, the peak position would have been at 2:1 ( $2I_2:1I^-$ ) and 3:1 ( $3I_2:1I^-$ ), respectively. In other words, the presence of these species would have shifted the peak position from 1:1. Our repeated experiments did not show any such shift to indicate the existence of polyiodide ions larger than  $I_3^-$  ions. It should be pointed out that the correction for iodine absorbance did not change the peak position in Figure 3. A small amount of asymmetry in this figure is presumably caused by an overcorrection from absorbance data obtained under high iodine concentrations. For example, for 8:2 (high iodine) and 2:8 (low iodine), data points we subtracted absorbance values of 0.032 ( $0.04 \times 8/10$ ) and 0.008 ( $0.04 \times 2/10$ ), respectively. The actual

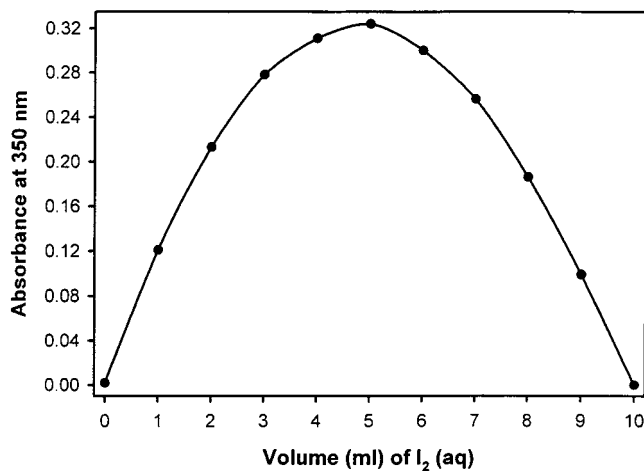


**Figure 3.** Job's method of continuous variation is applied to identify iodide species at 350 nm. The volumes of  $I_2$  and  $I^-$  ions of the same concentration ( $2.6 \times 10^{-4}$  M) were added in such a way as to get a total volume of 10 mL. The peak appears at 1:1 ratio of iodine and iodide ion, suggesting the formation of  $I_3^-$  species.

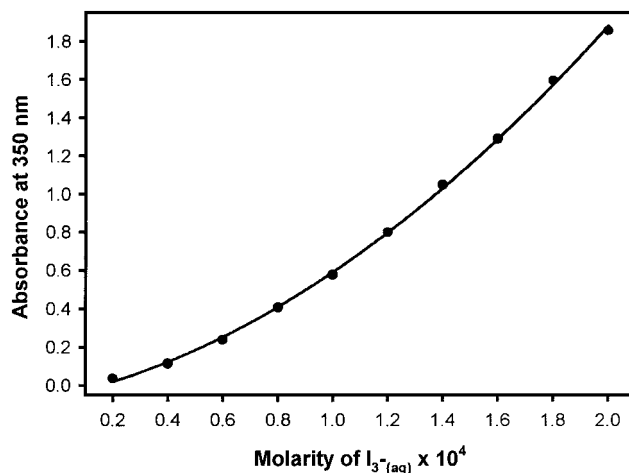


**Figure 4.** Molarity of  $I_3^-$  plotted against absorbance at 350 nm (15 °C). Unlike in Figure 2, a nonlinear relationship can be noticed at higher concentrations.

correction term should have been less than the above values as a part of iodine molecules will remain bonded to  $I^-$  ions. Since the correction term for 2:8 is already insignificant compared to that for 8:2, the above corrections result in an asymmetry in the figure. From the above analysis, we can say that the absorbance at 350 nm is almost solely due to  $I_3^-$  ions. Now, the valid question is, can there be other wavelengths at which the polyiodide ions  $I_5^-$  or  $I_7^-$  absorb? To search for this answer, we refer to Figure 1 and absorbance data of 1:1/4 and 1:1/2. One can notice that the absorbance at 350 nm is almost doubled as the proportion of iodide ion is doubled. Since the  $I_2$  concentration is fixed at  $2.0 \times 10^{-4}$  M, by doubling the  $I^-$  ion concentration from 1/4 to 1/2 of  $2.0 \times 10^{-4}$  M, the absorbance at 350 nm is expected to be doubled (also  $I_3^-$  concentration doubled) if all the  $I^-$  ions are involved with the triiodide ions. It should be mentioned that the  $I_3^-$  absorbance plot (Figure 4) is almost linear between the absorbance values of 0 and 0.8 and was obtained by saturating limiting amounts of iodine with excess of iodide ions (iodine concentration determined by thiosulfate titration). If reactions 2 and 3 indeed take place forming  $I_5^-$  and  $I_7^-$  ions, one would expect at least certain amounts of  $I^-$  ions involved with these species. Hence, by doubling the iodide ion concentration one would not expect a doubled amount of  $I_3^-$  ions or absorbance at 350 nm. Thus, the

TABLE 1: Optimized Bond Lengths, Angles, and Stabilization Energy (SE) Values Relative to Separated Molecules and Ions<sup>c</sup>

complex	bond lengths (Å)			bond angles (degrees)			energies (kcal/mol) (eV in parentheses)	
	O–H	I–I	O–I or H–I	H–I–I or O–I–I	H–O–I or I–H–I	I–I–I	SE	SE/I <sub>2</sub>
H <sub>2</sub> OI <sub>2</sub>	0.95	2.69	2.81	180	124		6.0	6.0
H <sub>3</sub> OI <sub>2</sub> <sup>+</sup>	0.96	2.68	2.48	104			10.0	10.0
	0.99							
I <sub>2</sub> OH <sup>−</sup>	0.95	3.24	2.06	179	114		88	88
I <sub>2</sub> H <sup>+</sup>		2.74	1.62	97			143	143
I <sub>4</sub> H <sup>+</sup>		2.68	1.69	98	177		151	76
		2.72	2.42	104				
I <sub>6</sub> H <sup>+</sup>		2.67	1.68	81	178	105	153	51
		2.72	2.48	97		108		
		3.88		104		177		
I <sub>8</sub> H <sup>+</sup>		2.67	1.68	81	178	99	155	39
		2.72	2.46	97		108		
		3.89		103		177		
		4.36						
I <sub>5</sub> <sup>−</sup> (C <sub>2v</sub> )		2.81				115	13 (0.56)	6.5
		3.17				179		
I <sub>5</sub> <sup>−</sup> (linear)		2.80				180	11	5.5
		3.17					(0.48)	
I <sub>5</sub> <sup>−</sup> (expt.)		2.81 <sup>a</sup>				95 <sup>a</sup>	(0.51) <sup>b</sup>	
		3.17 <sup>a</sup>				186 <sup>a</sup>		

<sup>a</sup> Reference 19. <sup>b</sup> Reference 17. <sup>c</sup> For I<sub>5</sub><sup>−</sup> ion the SE value is calculated relative to I<sub>3</sub><sup>−</sup> ion and I<sub>2</sub> molecule. The energy values are calculated at the MP2/LANL2DZ/HF/LANL2DZ level. The I–I shortest distances are corrected by −0.15 Å and longer ones by −0.10 Å.

present experimental results suggest the existence of only I<sub>3</sub><sup>−</sup> ions and no I<sub>5</sub><sup>−</sup> or I<sub>7</sub><sup>−</sup> ions in the solution.

**Evidence for Polyiodine Species in Solution.** By referring to reaction 1 and applying data from 1:1/2 and 1:1/4 molar ratio (I<sub>2</sub>:I<sup>−</sup>) experiments (Figure 1), we can postulate that as the I<sub>3</sub><sup>−</sup> ion concentration is decreased by 50% (from 1/2 to 1/4, assuming all I<sup>−</sup> ions taking part in the reaction), there should be a corresponding increase in the I<sub>2</sub> concentration by 50% as each I<sub>3</sub><sup>−</sup> ion is made up of one I<sub>2</sub> and one I<sup>−</sup> ion. The experimental absorbance (proportional to concentration) decrease at 350 nm is 45% (fairly close to 50%), whereas the absorbance increase at 460 nm is only 20%, that is, less than 1/2 of the decrease in the triiodide concentration. The above low percentage of I<sub>2</sub> concentration increase can be explained if we assume that a half of the increased number (45/2, around 22%) of I<sub>2</sub> is involved with other polyiodine species for which all the iodine molecules are not available as I<sub>2</sub> to give absorbance at 460 nm. Repeated experiments provided similar results, suggesting that some of the iodine molecules form clusters. The following theoretical studies were carried out to identify these species and examine their possible structures.

### Theoretical Results on Polyiodine Species

**Method Applied and Reliability.** The ab initio geometry optimizations were carried out at the Hartree–Fock level (HF) by applying the LANL2DZ basis set.<sup>16</sup> Each geometry optimization was followed by a single-point energy calculation at the MP2/LANL2DZ level. Since these ab initio calculations involved an effective potential for core electrons, validity of the method was examined by applying this basis set in known cases of iodine complexes. For example, the geometry optimization of I<sub>5</sub><sup>−</sup> ion provided both the linear as well as a bent geometry (close to C<sub>2v</sub> symmetry) and are comparable to those reported by Sharp and Gellene.<sup>15</sup> The stabilization energy (SE) value (relative to separated I<sub>3</sub><sup>−</sup> ion and I<sub>2</sub> molecule) for the more stable C<sub>2v</sub> structure (Table 1) is around 0.56 eV and is quite close to that of the experiment (0.51 eV).<sup>17</sup> The geometry optimization of I<sub>2</sub> molecule resulted in an I–I distance of around 2.82 Å and is longer than the experimental length<sup>18</sup> by around 0.15 Å.

This length correction when applied to the shorter I–I distance in the calculated I<sub>5</sub><sup>−</sup> structure, an I–I bond length quite close to the experimental value<sup>19</sup> was obtained. Similarly, by comparing the calculated structural features for I<sub>5</sub><sup>−</sup> ion with those of the experimental values we determined another correction factor of −0.10 Å for the longer I–I distance. These length corrections are applied in reporting the I–I distances (Table 1) in the optimized iodine and polyiodine complexes (Figure 5).

**Geometry Optimization and Energy Calculations.** *I<sub>2</sub> Complex with H<sub>2</sub>O.* We first tried geometry optimization of I<sub>4</sub>, I<sub>6</sub>, etc. species with linear and nonlinear starting geometries. None of them provided a stable structure relative to separated I<sub>2</sub> molecules. Then, we tried possible complexes with H<sub>2</sub>O and obtained a complex that involves only a single iodine molecule per water molecule (H<sub>2</sub>OI<sub>2</sub> complex) with a SE (stabilization energy) value of around 6.0 kcal/mol relative to separated molecules. In this complex, the I<sub>2</sub> molecule is linearly oriented with the O atom of the H<sub>2</sub>O molecule. We could not obtain a stable structure for H<sub>2</sub>OI<sub>4</sub>, H<sub>2</sub>OI<sub>6</sub>, etc. involving more than one iodine molecule. Figure 5 presents the H<sub>2</sub>OI<sub>2</sub> geometry and is very similar to what we reported earlier.<sup>20</sup>

*I<sub>2</sub> Complexes with H<sub>3</sub>O<sup>+</sup>, H<sup>+</sup>, and OH<sup>−</sup> Ions.* Next, we tried ionic complexes of iodine with H<sub>3</sub>O<sup>+</sup>, H<sup>+</sup>, and OH<sup>−</sup> ions that are available in an aqueous solution. Among the ionic complexes of the I<sub>2</sub> molecule, the I<sub>2</sub>H<sup>+</sup> is most stable with an SE value of around 143 kcal/mol (Table 1) followed by I<sub>2</sub>OH<sup>−</sup> (SE = 88 kcal/mol) and H<sub>3</sub>OI<sub>2</sub><sup>+</sup> (SE = 10.0 kcal/mol) complexes. In the H<sub>3</sub>OI<sub>2</sub><sup>+</sup> ion, the I<sub>2</sub> molecule is bonded through an H atom rather than an O atom even when the starting geometry had an O–I bonding. The H–I distance in this complex is around 2.48 Å and is longer than a regular H–I bond of 1.61 Å in the gaseous HI molecule.<sup>18</sup> The H–I–I angle in this complex is around 104° representing a nonlinear arrangement of the iodine molecule with the H atom. In the I<sub>2</sub>OH<sup>−</sup> ion, the I<sub>2</sub> molecule is bonded through the O atom and is linearly arranged with the O atom (O–I distance of around 2.06 Å). The I–I distance in this ion is around 3.24 Å and is significantly longer than a regular I–I distance in the I<sub>2</sub> molecule. The Mulliken charge distribution at this level of calculation suggests that the −1 charge on the

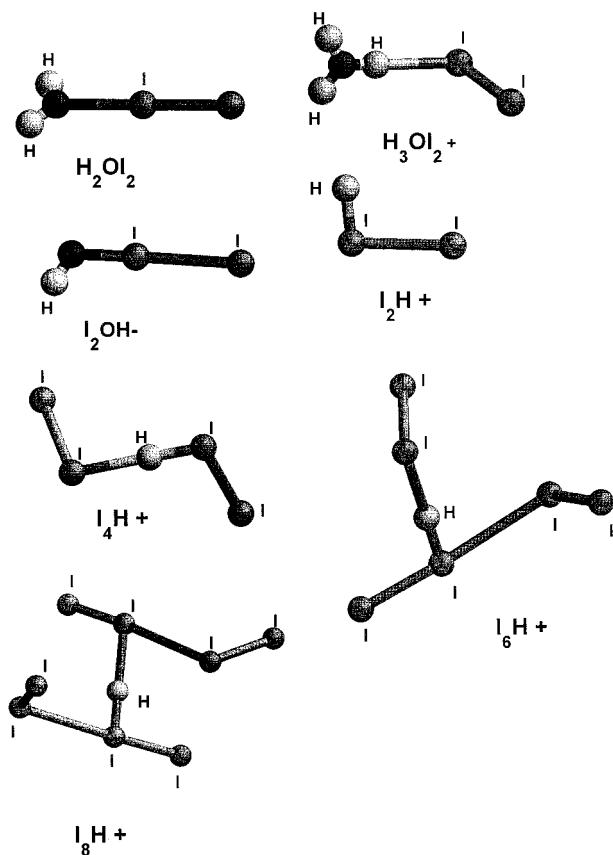


**Figure 5.** Optimized structures of different  $I_2$ ,  $I_4$ ,  $I_6$ , and  $I_8$  complexes are presented. The optimization was done at the HF/LANL2DZ level by using the Gaussian 94 series of programs.

$I_2OH^-$  ion is almost equally divided between OH (charge  $-0.56$ ) and  $I_2$  ( $0.44$ ) with a slightly larger charge on OH. The  $I_2H^+$  ion has a nonlinear geometry with an I–I distance of around  $2.74$  Å and is slightly longer than a regular I–I distance. These structural features are presented in Table 1.

*Polyiodine Species: Other  $I_{2x}$  Complexes ( $x = 2, 3, 4, etc.$ ) with  $H^+$ .* Since the  $H^+$  ion provides the most stable  $I_2$  complex ( $I_2H^+$ ), we examined only the protonated structures for  $I_4$ ,  $I_6$ , and  $I_8$  clusters. The starting structures involved a number of assumed geometries, most of which resulted in unstable complexes. The stable  $I_4H^+$ ,  $I_6H^+$ , and  $I_8H^+$  structures are presented in Figure 5 and have SE values (for singlet states) of around 151, 153, and 155 kcal/mol, respectively, relative to separated  $I_2$  molecules and  $H^+$  ion. An analysis of Mulliken charges suggests that the  $+1$  charge originally on  $H^+$  ion is distributed to other centers in the optimized structure. The SE/ $I_2$  values for  $I_2H^+$ ,  $I_4H^+$ ,  $I_6H^+$ , and  $I_8H^+$  are 143, 76, 51, and 39 kcal/mol, respectively, and suggest that the increase in the SE value with successive addition of  $I_2$  is substantially decreased. Hence, much larger cluster formation of this type may not be possible. The structural features of various clusters are presented in Table 1 together with their energy values.

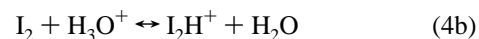
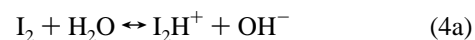
In the  $I_4H^+$  complex, the  $H^+$  ion binds two  $I_2$  molecules (through two I atoms) on opposite sides with the I–H–I angle of around  $177^\circ$  and H–I–I angles of around  $98^\circ$  and  $104^\circ$ . One of the bonded H–I lengths is significantly longer ( $2.42$  Å) than the other one ( $1.69$  Å). The I–I distances in two bonded  $I_2$  molecules are  $2.68$  and  $2.72$  Å and are very close to the regular I–I distance in a gaseous iodine molecule. Interestingly, our starting geometry had two iodine molecules arranged linearly with the  $H^+$  ion in the middle, and the optimized structure, as

can be noticed in Figure 5, is quite different from the starting geometry.

In the  $I_6H^+$  complex, all three  $I_2$  molecules are not directly bonded to the  $H^+$  ion. Rather, two are bonded (I–I distances  $2.67$  and  $2.72$  Å) to the  $H^+$  ion through their I atoms (H–I distance of around  $1.68$  and  $2.48$  Å), and the third  $I_2$  molecule is bonded to an iodine molecule at an I–I distance of around  $3.88$  Å. This distance is too large to provide a strong bonding between the third iodine molecule and the rest of the  $I_6$  complex. The I–I distance in the third  $I_2$  molecule is around  $2.67$  Å and is close to those that exist in other iodine molecules within this complex. The starting geometry had a trigonal planar arrangement of iodine molecules with the proton in the middle, and the optimized structure as shown in the figure is quite different from this assumed geometry.

Similarly, in the  $I_8H^+$  complex, the starting geometry had a tetrahedral arrangement of four iodine molecules around the proton. The optimized structure in this case is also quite different from the starting geometry with only two  $I_2$  molecules directly bonded to the proton. This part of the structure is very similar to that noticed in the  $I_4H^+$  cluster. Each of the other two  $I_2$  molecules is bonded to its nearest neighbor iodine molecule at a fairly large distance (I–I distance  $3.89$  and  $4.36$  Å). At this large inter-iodine distance, the bonding is expected to be quite weak and this complex is expected to break down quite readily into smaller  $I_4H^+$  species. The I–I distance in four  $I_2$  molecules within the complex ranges from around  $2.67$  to  $2.72$  Å and is close to that of a regular gas-phase iodine molecule. The H–I distances ( $1.68$  and  $2.46$  Å) are about the same as those noticed in  $I_4H^+$  and  $I_6H^+$  clusters (Table 1). There are three distinct I–I–I angles of  $99^\circ$ ,  $108^\circ$ , and  $178^\circ$  and H–I–I angles of  $81^\circ$ ,  $97^\circ$ , and  $103^\circ$ . Two of the H–I–I angles are very close to those observed in an  $I_4H^+$  cluster and suggest a structural similarity between the  $I_4H^+$  and other larger clusters ( $I_6H^+$  and  $I_8H^+$ ).

**Heat of Reaction ( $\Delta H$ ) for  $I_2H^+$  Formation.** Two possible reactions are considered that may form  $I_2H^+$  ions in the solution:



The gas-phase heat of reaction at 298 K is given by the following expression:

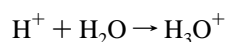
$$\Delta H = \Delta E (\text{electronic}) + \Delta E (\text{thermal}) + \Delta nRT$$

The first energy term includes the electronic energy change (products–reactants) at 0 K and the change in electronic energy difference from 0 to 298 K (considered to be zero here). For reactions 4a and 4b, the  $\Delta E$  (electronic) values are 268 and 36 kcal/mol, respectively. The second term includes the zero-point energy and vibrational, rotational, and translational energy terms. The  $\Delta n$  represents the difference between the number of product and reactant molecules, which is 0 in this case. The thermal energy values are obtained from the frequency calculations of the optimized structures. The  $\Delta H$  values after correcting for the basis set superposition errors (BSSE) are 265 and 31 kcal/mol, respectively, for reactions 4a and 4b. The BSSE for  $H_3O^+$  and  $I_2H^+$  were calculated by applying the counterpoise method<sup>21</sup> in which the basis set of H was included during the energy calculation of the  $H_2O$  and  $I_2$  molecules. The corrections needed (compared to uncorrected values) were by 2.24 and 2.44 kcal/mol, respectively. The above  $\Delta H$  or  $\Delta E$  values suggest that very little energy is required for the  $H^+$  ion transfer from  $H_3O^+$  ion to  $I_2$  molecule in the gas phase (reaction 4b). We also examined



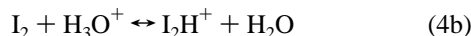
the solvation or dielectric effect for reactions 4a and 4b by applying the Onsager reaction field method. While there was almost no change in the  $\Delta E$  value for reaction 4a (269 kcal/mol), there was a decrease by about 4 kcal/mol for reaction 4b (32 kcal/mol). Thus, the reaction 4b can be considered to take place predominantly in the solution. The reaction 4a, however, cannot be ignored solely on enthalpy grounds. For a comparison, the reaction between two water molecules forming a hydronium ion and a hydroxide ion can be considered. The calculated  $\Delta H$  value for this reaction is quite large (234 kcal/mol, with solvation 236 kcal/mol), and still the reaction takes place to a small extent ( $10^{-7}$  M). A greater stabilization arising from H-bonding of ionic species presumably allows this reaction to happen. A similar argument can also be made in favor of reaction 4a.

At this point we can examine the accuracy of energy values for protonated species (at this level of theory) by calculating the proton affinity (PA) value for  $\text{H}_2\text{O}$  molecule at 298 K and comparing it with the experimental value.<sup>22</sup> The PA value is obtained by calculating the  $\Delta H$  value for the following reaction:



The  $\Delta E$  (electronic) value for this reaction (with BSSE correction) is 176.72 kcal/mol. The  $\Delta E$  (thermal) includes translational energy for the  $\text{H}^+$  ion ( $3/2RT$ ), translational, rotational, vibrational, and zero-point energy terms for  $\text{H}_3\text{O}^+$  and  $\text{H}_2\text{O}$  molecules. The  $\Delta nRT$  value in this case is  $-0.59$  kcal/mol ( $\Delta n = -1$ ) and the  $\Delta H$  value (PA), thus calculated, is around 169 kcal/mol and is fairly close to the experimental value of  $166.5 \pm 2$  kcal/mol.<sup>22</sup>

**Possible Mechanism of Iodine Cluster Formation.** We put forward the following mechanism for the cluster forming reaction on the basis of the present study:



Since only a small quantity of  $\text{H}_2\text{O}$  undergoes autodissociation to  $\text{H}_3\text{O}^+$  and  $\text{OH}^-$  ions, the  $\text{I}_2\text{H}^+$  or other similar species can have a substantial concentration at a relatively large concentration of iodine. A large concentration of  $\text{I}_2$  favors product formation by shifting equilibrium reactions 4–7 to the product side (Le Chatelier's principle). Hence, these cluster formations are expected to be more dominant at higher concentrations of iodine as was noticed in our experiment.

**pH of Iodine Solution and Verification of Cluster Forming Mechanism.** One may expect that the reactions 4–7 will increase the pH of a solution as they increase the hydroxide ion or decrease the hydronium ion concentration in the solution. However, there are two other reactions (reactions 8 and 9) that need to be considered at this time. These reactions tend to decrease the pH by decreasing the hydroxide ion or increasing the hydronium ion (or  $\text{H}^+$ ) concentration in the solution.

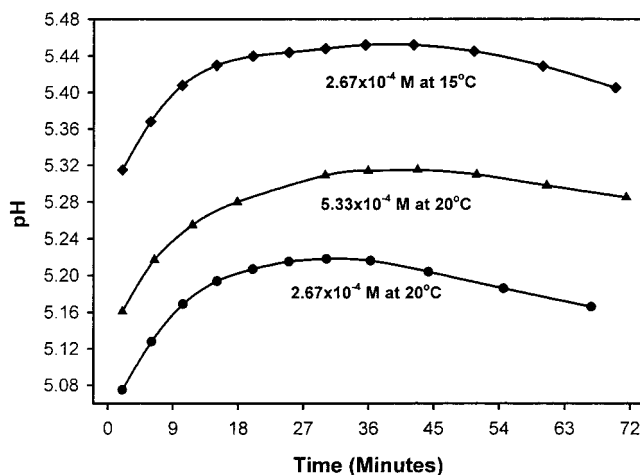
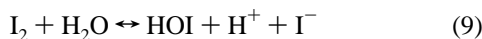
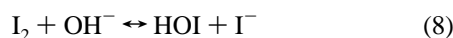


**Figure 6.** Time-dependent variation of pH of iodine solutions at 15 and 20 °C. The bottom two curves represent the solutions at 20 °C with iodine concentrations of  $2.67 \times 10^{-4}$  and  $5.33 \times 10^{-4}$  M  $\text{I}_2$ , respectively, and the top curve represents the iodine concentration of  $2.67 \times 10^{-4}$  M  $\text{I}_2$  at 15 °C.

Thus, the pH of an iodine solution will depend on all these reactions (4–9) and the overall concentrations of  $\text{H}^+$  or  $\text{OH}^-$  ions in the solution. When an acid is added to the solution (pH is decreased), the concentrations of  $\text{I}_2\text{H}^+$  and  $\text{I}_2$  (free) are expected to increase (Le Chatelier's principle applied to eqs 4a, 4b, 8, and 9). It is expected that both  $\text{I}_2\text{H}^+$  and  $\text{I}_2$  will absorb close to the same wavelength (460 nm), as in most iodine complexes the spectrum is primarily due to electron transition within iodine atoms.<sup>20,23</sup> From eqs 8 and 9, we would also expect a decrease in the  $\text{I}^-$  ion concentration and hence the  $\text{I}_3^-$  concentration that absorbs at 350 nm. Indeed, the absorbance of  $\text{I}_2/\text{KI}$  solution is increased at 460 nm and decreased at 350 nm when an acid is added to the solution. These results are consistent with the reactions presented above.

Figure 6 shows how the pH of aqueous solutions of iodine changes with time. The bottom two curves represent the solutions with iodine concentrations of  $2.67 \times 10^{-4}$  and  $5.33 \times 10^{-4}$  M  $\text{I}_2$ , respectively (determined by thiosulfate titration), at 20 °C, and the uppermost curve represents the iodine solution of  $2.67 \times 10^{-4}$  M  $\text{I}_2$  at 15 °C. As one can notice, in each case the pH first increases and then gradually decreases with time. For the lower iodine concentration at 20 °C, the decrease in pH is more remarkable than that for the higher concentration. The faster protonation reactions (eqs 4–7) presumably result in an increased pH at the beginning. After some time, the effect of the hydrolysis reaction of iodine (that decreases pH, eqs 8 and 9) becomes significant when the protonation reactions are no longer dominant and the pH is decreased. At a higher iodine concentration, when the cluster formation among the  $\text{I}_2$  molecules becomes more favored, reactions 4–7 become more dominant causing a larger increase in the pH value. Similarly, at a lower temperature (15 °C), the iodine clusters are expected to be more stable and may be present in a larger number giving a larger increase in the pH value compared to the higher temperature curve of same concentration. Hence, the time-dependent pH variation of iodine solution can be well-explained on the basis of our postulated cluster forming (eqs 4–7) mechanism and the iodine hydrolysis reactions (eqs 8 and 9).

#### Ambiguities in Earlier Determination of $\text{I}_5^-$ Ions in the AI Complex

About 20 years ago, Teitelbaum et al.<sup>4</sup> suggested the presence of  $\text{I}_5^-$  ions within the amylose–iodine (AI) complex cavity on

the basis of certain similarities between the spectrum of trimesic acid–iodine (TMAI) complex (known to contain  $I_5^-$  ions) and that of the AI complex. A closer examination of peak positions and intensities suggests that a significant dissimilarity exists between the AI and the TMAI spectra, and raises question about the reliability of the  $I_5^-$  ion identification within the AI complex. For example, the resonance Raman spectrum<sup>4</sup> due to AI complex shows peaks at 163, 109, and 56  $cm^{-1}$ , and the TMAI complex shows peaks at 162, 104, and 75  $cm^{-1}$ . The third peak, certainly, does not appear at the same location in these complexes. Second, the intensities of the last two peaks are too low (please see Teitelbaum et al.'s Figure 5, parts a and b) in the TMAI complex to be comparable with those in the AI complex. Similarly, the Mössbauer spectrum due to the TMAI complex shows relative intensities of 2:1:1 in sites 1, 2, and 3, respectively, and are different from those obtained for the AI complex prepared in a standard (adding KI) method (2:2:1) or in a vapor method (2:2:0.5). Thus, a strong resemblance between the resonance Raman or Mössbauer spectrum of the TMAI complex and that of the AI complex is not there to justify the consideration of the same  $I_5^-$  chromophore unit in both the complexes. It should be pointed out that the spectrum due to AI complex prepared in a standard method must be identical to that of the complex prepared from iodine vapor as an identical complex is formed in each case. While the resonance Raman spectrum shows this identity, the Mössbauer spectrum shows significant discrepancies by having or not having a site 4. Even though the authors<sup>4</sup> tried to explain these discrepancies by stating possible differences in the  $I_5^-$  microenvironment, the above results (which should have been identical) cast doubt about the reliability of the Mössbauer method in identifying the iodine chromophore unit within the AI complex.

The electronic absorption spectrum<sup>5</sup> for the AI complex (300 K) shows a major peak at around 17 000  $cm^{-1}$  with a low-frequency peak at around 14 000  $cm^{-1}$ . In contrast, the major peak for the TMAI complex appears at around 14 000  $cm^{-1}$  (no peak at 17 000  $cm^{-1}$ ) with almost no low-frequency structure at this temperature. At 85 K, however, the TMAI complex spectrum shows a low-frequency structure at around 10 000  $cm^{-1}$  with the major peak still at around 14 000  $cm^{-1}$ . Hence, we can say that the experimental evidence is not strong enough to assume the same chromophore in both TMAI and AI complexes. Thus, the identification of  $I_5^-$  chromophore within the AI complex cannot be supported by a strong spectral similarity between the AI and TMAI complexes.

Three possible sources of  $I_5^-$  ions are suggested in Teitelbaum et al.'s<sup>4</sup> paper. First, an iodide ion may first form as a result of a hydrolysis reaction of iodine, which then enters into the cavity of amylose helix and forms an  $I_5^-$  ion by combining with two iodine molecules. The second possibility is that the  $I_5^-$  ion may first form in the solution and then become bonded to the amylose helix, and the third possibility suggests the formation of  $I_5^-$  ion in the presence of amylose. Since in our recent ISE experiments<sup>8</sup> (discussed above) we did not notice any change in the iodide ion concentration even when amylose was added, we seriously doubt whether the AI complex can at all involve any iodide ion, including the  $I_5^-$  ion.

### Concluding Comments

The aqueous solution of iodine in the presence of KI forms  $I_3^-$  ions and a number of protonated polyiodine complexes.

There is no experimental evidence to support the formation of  $I_5^-$  or  $I_7^-$  ions in the solution. It may not be surprising as the SE value for the  $I_3^-$  ion is significantly larger (30.2 kcal/mol<sup>17</sup>) than that of an  $I_5^-$  ion (11.8 kcal/mol<sup>17</sup>). Similar results are also expected for an  $I_7^-$  ion. Our results also suggest that the straight line relationship in Figure 2 is due to  $I_2$  and  $I_2H^+$ . The larger iodine species, like  $I_4H^+$ ,  $I_6H^+$ , etc., do not absorb at 460 nm. This is why we could not account for all the iodine molecules on the basis of absorbance at 460 nm. That is, when the  $I_3^-$  concentration was decreased by 50%, the absorbance due to  $I_2$  and  $I_2H^+$  was increased by only 20% (not 50%) as the rest of the iodine molecules were involved with larger clusters that do not absorb at 460 nm. It seems that the concentration of species such as  $I_4H^+$ ,  $I_6H^+$ , etc. are increased together with  $I_2$  and  $I_2H^+$  as total iodine concentration is increased in the solution. Thus, a linear increase in  $I_2$  and  $I_2H^+$  concentration (hence, absorbance at 460 nm in Figure 2) is maintained even when the larger species are formed in the solution.

**Acknowledgment.** We acknowledge a research development grant from Penn State, DuBois Educational Foundation, and generous computation time on SP2 system from Numerically Intensive Computation group at the center for Academic Computing. We also acknowledge helpful discussions with Doug Fox of Gaussian Inc. and Peter Gold of Penn State.

### References and Notes

- (1) Lambert, J. L. *Anal. Chem.* **1951**, *23*, 1251.
- (2) Lambert, J. L.; Zitomer, F. *Anal. Chem.* **1963**, *35*, 405.
- (3) Teitelbaum, R. C.; Ruby, S. L.; Marks, T. J. *J. Am. Chem. Soc.* **1978**, *100*, 3215.
- (4) Teitelbaum, R. C.; Ruby, S. L.; Marks, T. J. *J. Am. Chem. Soc.* **1980**, *102*, 3322.
- (5) Mulazzi, E.; Piseri, L.; Pollini, I.; Tubino, R. *Phys. Rev. B* **1981**, *24*, 1429.
- (6) Cesaro, A.; Jerian, E.; Saule, S. *Biopolymers* **1980**, *19*, 1491.
- (7) Minick, M.; Fotta, K.; Khan, A. *Biopolymers* **1991**, *31*, 57.
- (8) Calabrese, V. T.; Khan, A. *J. Polym. Sci. A* **1999**, *37* (15), 2711.
- (9) Hach, R. J.; Rundle, R. E. *J. Am. Chem. Soc.* **1951**, *73*, 4321.
- (10) James, W. J.; Hach, R. J.; French, D.; Rundle, R. E. *Acta Cryst.* **1955**, *8*, 814.
- (11) Havinga, E. E.; Wiebenga, E. H. *Acta Cryst.* **1958**, *11*, 733.
- (12) Herbstein, F. H.; Kapon, M. *Acta Crystallogr. Sect. A* **1972**, *28*, 574.
- (13) Herbstein, F. H.; Kapon, M. *Nature* **1972**, *239*, 153.
- (14) Herbstein, F. H.; Kapon, M.; Reisner, G. M. *Proc. R. Soc. London A* **1981**, *376*, 301.
- (15) Sharp, S. B.; Gellene, G. L. *J. Phys. Chem. A* **1997**, *101*, 2192.
- (16) (a) Frisch, M. J. et al. *Gaussian 94*; Gaussian Inc.: Pittsburgh, PA, 1995. (b) Hay, P. J.; Wadt, W. R. *J. Chem. Phys.* **1985**, *82*, 299 (LANL2DZ basis set).
- (17) Quoted from ref 15.
- (18) Huber, K. P.; Herzberg, G. *Constants of Diatomic Molecules* Van Nostrand Reinhold: New York, 1979.
- (19) Broekema, J.; Havinga, E. E.; Wiebenga, E. H. *Acta Crystallogr.* **1957**, *10*, 596.
- (20) Fonslick, J.; Khan, A.; Weiner, B. *J. Phys. Chem.* **1989**, *93*, 3836.
- (21) Boys, S. F.; Bernardi, F. *Mol. Phys.* **1970**, *19*, 553.
- (22) Lias, S. G.; Liebman, J. F.; Levin, R. D. *J. Phys. Chem. Ref. Data* **1984**, *13* (3), 695.
- (23) Khan, A. *J. Chem. Phys.* **1992**, *96*, 1194.